Influence of thermoplastic interleaves and its healing effect on the failure mechanisms of open-hole notched composite laminates

Tianqi Zhang, Mehdi Yasaee

PII: S0266-3538(22)00339-6

DOI: https://doi.org/10.1016/j.compscitech.2022.109597

Reference: CSTE 109597

To appear in: *Composites Science and Technology*

Received Date: 1 April 2022

Revised Date: 15 June 2022

Accepted Date: 16 June 2022

Please cite this article as: Zhang T, Yasaee M, Influence of thermoplastic interleaves and its healing effect on the failure mechanisms of open-hole notched composite laminates, *Composites Science and Technology* (2022), doi: https://doi.org/10.1016/j.compscitech.2022.109597.

Control

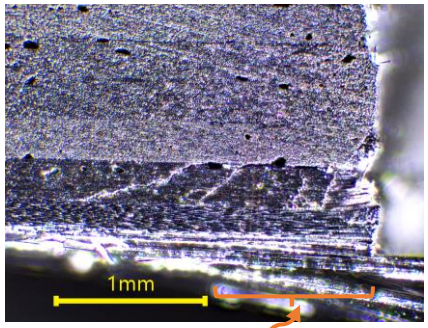

+45° ply peeling (1.07mm)

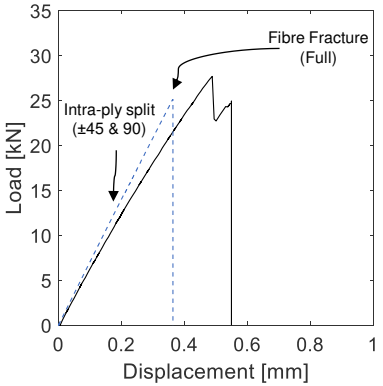

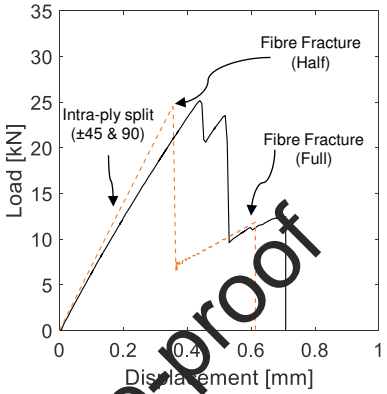

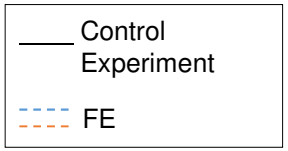

Control open-hole failure sequence:

1. Ply splits (matrix cracks)
2. Delamination + fibre fracture

Interleaved

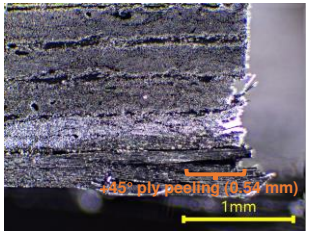

Interleaved sample with damage at drill site

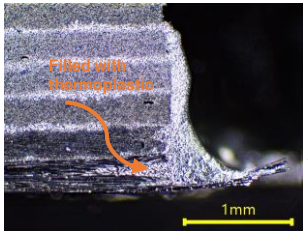

Re-heated interleaved sample with damage at drill site healed

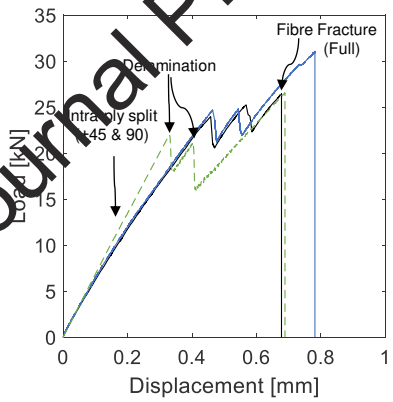

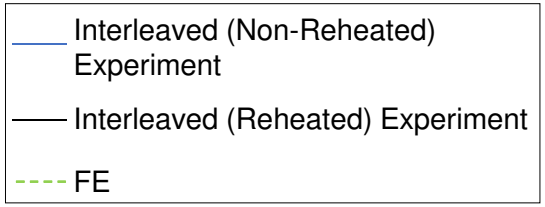

Interleaved open-hole failure sequence:

1. Ply splits (matrix cracks)
2. Delamination
3. Fibre fracture

Composites Science and Technology, Volume 227, August 2022, Article number 109597
DOI:10.1016/j.compscitech.2022.109597

Influence of thermoplastic interleaves and its healing effect on the failure mechanisms of open-hole notched composite laminates

Tianqi Zhang[1], Mehdi Yasaee[1*]

[1] School of Aerospace, Transport and Manufacturing, Cranfield University, MK43 0AL, UK.

*corresponding author: m.yasaee@cranfield.ac.uk

Abstract: This paper has explored the effect of thermoplastic interleaves on the mechanical performance of open-hole notched Carbon Fibre Reinforced Polymer (CFRP) composites. A fully verified FE model was produced to replicate the experimental results, as well as to study the sensitivity of the interlaminar properties on the open hole tensile failure mechanism sequence. Both experimental and numerical analysis results show that, the failure mechanisms and sequences are closely linked to the interfacial toughness, strength, and stiffness. With the addition of thermoplastic interleaves, the higher interfacial fracture toughness allows for a stable and gradual delamination growth. This effect lowered the interfacial strength, thereby releasing stress concentrations at the open-hole site. These features result in the higher overall load carrying capacity. A healing treatment on the thermoplastic interleaves post drill operation was conducted and assessed their effectiveness to fix the drill-induced damage through detailed microscopy inspections, to understand the condition of specimens' interfaces before and after the healing treatment. In comparison to non-healing treated interleaved sample, the healing treatment increased the tensile strength of the sample with the failure sequence changed.

Keywords: Carbon fibres – A; Delamination – B; Fracture toughness – B; Interfacial strength – B; Finite element analysis (FEA) – C;

1 Introduction

Fibre Reinforced Polymer (FRP) composites or specifically Carbon Fibre Reinforced Polymer (CFRP) composites have become increasingly popular in high performance engineering fields such as the aerospace and the motorsports industries. In comparison to the conventional metallic materials, CFRP composites have advantages of being lighter whilst possessing better corrosion resistance and fatigue performance with comparable strength and stiffness. In many cases, composite components will need to be physically joined to other components. To utilise fasteners for joints, open holes will need to be drilled. Apart from the additional stress concentration around the hole, the drilling process will introduce fracture and small delamination around the drill site [1]. For this reason, open-hole notched composites' residual strength and its failure mechanism has been subject to extensive studies.

Wisnom et al. [2][3] investigated the scaling effects and the correspondent failure mechanisms in open hole tension (OHT) tests for quasi-isotropic laminates. The size effects of thickness and open-hole diameter were shown to affect the open-hole strength. In the study, the failure mechanisms of notched composites were classified into three types: Pull-out failure, which is a sequence of 0° fibre fracture and delamination which results in sections of the ±45° layers to pull-out from adjacent halves of the laminate; Brittle failure, where a clean fracture occurs across the full width/thickness without much delamination; Delamination failure, which show large scale delamination and ply split before the fibre fracture.

Hallett et al. [4] used numerical analysis approach to simulate the failure mechanism and overall behaviour of open-hole notched composites. They showed that to get an accurate strength prediction from the FE simulation, a Weibull statistical approach is required to correctly adjust from the model prediction to that of the real structure. It is evident from these numerical studies that in order to get accurate representation of the failure mechanisms of

notched composites, the simulation must be capable to model laminate ply splitting (matrix cracks), fibre fracture, and inter-laminar failures (delamination) correctly.

The initial quality of the open-hole notched composites is closely linked to the manufacturing process. The drilling induced damage such as burrs, tearing, and delamination [1] are of concern due to their potential influence to the integrity of composites. It was identified that the drilling induced damage is predominantly caused by the peeling force and the thrust force from the drill bit. It usually occurs at the top and the back surface around the drilled hole, thus they are named as peel-up delamination and push-out delamination, respectively [5]. Xu *et al.*[1] carried out the experimental investigation of the drilling-induced defects on CFRP by ultrasonic C-scan and digital microscopy inspection. A novel delamination assessment criterion was developed to evaluate the damage severity. The drilling quality can be determined by the feed rate, spindle speed, and geometry of drill bit, this has been reviewed by Liu [6].

Academia and industries have never stopped seeking for toughening approaches to enhance the mechanical performance of composites [7]. Increasing the interlaminar toughness of the laminate may help improving the open hole strength of laminated FRP composites. Interleaving of laminated composites using various types of materials such as thermoset films, chopped fibres, particulate or thermoplastic films have been shown to be effective for improving the interlaminar fracture toughness of the host composite laminate [8][9]. Examples of interleaf materials that has been shown to be quite effective at increasing the interlaminar toughness are thermoplastic interleaves [8][9][10][11]. What makes this material quite unique, is the ability to re-heat and reform the film to re-bond the interlaminar regions once delamination has already formed. Wang et al. [12] showed the original toughness of the interlaminar interface can be recovered after delamination by as much as 88% and 36% for mode I fracture toughness and shear strength, respectively. Different thermoplastic interleaves may be used for this purpose, so long as the melting temperature remain low enough not to cause concern with regards to the

thermal degradation of the thermoset matrix of the host composite. The extended bridging zone and the torturous crack path of the interleaved interface are recognized as the main factors of the interfacial toughness enhancement [13] [9]. Thermoplastic Polyurethane (TPU) [14], Poly(ethylene-co-methacrylic acid) (EMAA) [12], Polyethersulfone (PES) [15] have been shown to produce significant increase in both Mode I and Mode II fracture toughness of CFRP composites. For thermoplastic films that may be incompatible with the matrix resin of the composite laminate, suitable surface treatment (e.g. plasma treatment) may be applied to activate the surface for improved adhesion [16,17]. Use of thermoplastic interleaves to improve the open-hole notched strength of a laminated composites has not been studied in detail previously.

While substantial efforts and progress have been made to characterise the fracture toughness enhancement of composites with interleaving material, little has been done to understand the toughening performance to the structural composite component. In this paper, an experimental study is presented to explore the influence of thermoplastic interleaves on the open-hole strength. The effect of re-healing will be assessed to identify whether any strength recovery can be achieved by healing drill induced damages. Using the experimental results, numerical FE models will be produced and verified to further investigate how interfacial properties change the failure mechanisms of open-hole composites.

2 Materials and experimental procedures

2.1 Tensile test

Quasi-isotropic $[45/90/-45/0]_S$ laminates are manufactured with unidirectional XC-130 carbon fibre prepreg (Easy Composites Ltd. UK) consisting of Toray T700 24K UD carbon fibres, with Toray 250F epoxy resin. The material properties of fibres are presented in Table 1. Interleaved specimens were produced by embedding Thermoplastic Polyurethane (TPU) films

of 50 μm thickness (Shenzhen Tunsing Plastic Product Co., Ltd.) along each ply interface, material properties of interleaf are listed in Table 3. Interleaves were positioned with the assistance of laser projection to ensure the consistent location of the interleaved region in each layer and each batch. Both control and interleaved samples were vacuum cured in a convection oven at 120°C for 1 hour according to the manufacture's recommendation.

The cured panels were machined into individual specimens using CNC router and carbide milling bit with 4 mm diameter holes drilled using high hardness carbide drill bit also on the CNC router. The positional tolerance of the holes was approximately ±0.05 mm in the specimen's width direction. Overall, three batches were produced, one control and two interleaved with six sample repeats machined from each batch. From the two interleaved batches, one batch was subject to reheating treatment post drilling. This was conducted by using small 3 mm thick steel plates placed on both sides of the sample, on the open hole area, with pressure applied using a G-clamp and re-heated for 30 minutes at 150°C [12]. This reheating temperature was selected to ensure the interleaves reached low enough viscosity to re-distribute inside the laminate and into the damaged regions. However, a lower reheating temperature (equal to or below the maximum cure temperature e.g. 130°C in this case) may be applied for future studies so long as it is higher than the melting temperature of thermoplastic interleaves. This will reduce the risk of overheating the thermoplastic material as well as the composite laminate and remove the (minor) risk of material degradation due to thermal ageing. Earlier conducted trial tests on smaller samples showed very little scatter in the data and qualitative assessment of the post tested samples showed almost identical damage profile. Therefore, decision was made not to conduct close monitoring of the clamping pressure, however future investigations on this topic may benefit from closer detailed study on the clamping pressure on the quality of the re-heating treatment. The control samples had a nominal

thickness of 2.39±0.01 mm whilst the interleaving area of the non-reheated and reheated samples had the average thickness of 2.75±0.01 mm and 2.60±0.02 mm, respectively.

The geometry of the open-hole specimen is shown in Fig.1, which were designed in-line with the guidelines in ASTM-D3039 and ASTM-D5766 [18][19].

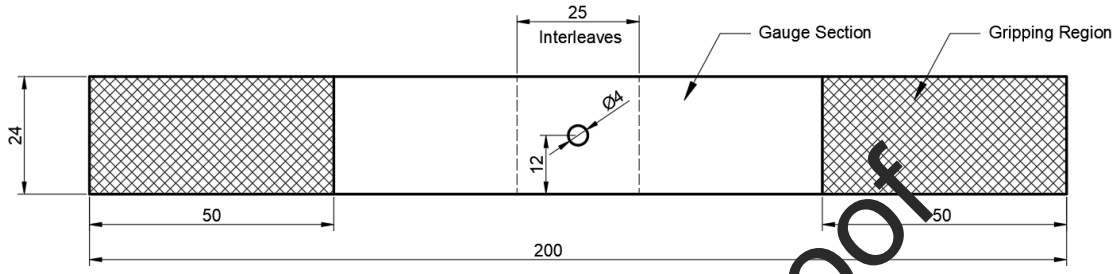

Fig.1 Open-hole specimen configuration (Unit: mm)

Table 1 Fibre properties (Toray T700) [20]

Fibre Tensile Modulus	230	GPa
Fibre Tensile Strain	2.1%	

Table 2 Properties of unidirectional CFRP laminate (1 = fibre direction) [20] [21] [22] [23]

E1	135	GPa
E2	7.00	GPa
G12	3.90	GPa
G23	2.96	GPa
v12	0.35	
Tensile strength (Xt)	2550	MPa
Fibre volume fraction	60%	
Prepreg areal weight	300	g/m^2
Cured ply thickness	0.3	mm

Table 3 Properties of thermoplastic interleaf (TPU) [24]

Melting temperature	100°C	
Melt Flow Index (ASTM-D1238-04)	12±5	g/10 min
Hardness (Shore A)	84±3	
Thickness	50	μm

2.2 Experimental procedure

An Instron universal test machine with 50kN loading cell was used to generate quasi-static tensile load at a displacement rate of 2 mm/min. A 3D Digital Image Correlation (DIC) system

from Dantec Dynamics was used to record the strain distribution and measure the displacement for each test. An area of 24 mm (Width)×40 mm (Height) on the specimen, which has the open hole in the central position, was picked as the region of interest (ROI) for the DIC cameras with recording of the test conducted at a frequency of 5 Hz. The displacement was measured from the DIC software between two points which has an initial distance of 36.6 mm, as shown in Fig.6, positioned to be in the middle of the specimen. This distance was selected as it was the furthest point away from the hole centre on the sample where the DIC image was captured.

2.3 Microscopy

To conduct cross-sectional microscopy, one un-tested specimen from each batch were cut at the middle length position and diamond polished as shown in Fig.2 . Cross sections of both (interleaved and non-interleaved) specimens were inspected by Swift trinocular optical microscope (SW380T) with magnifications of 4 and 10 times, to investigate the condition of the hole post-drilling and the cured interleave thickness distribution.

The interface structure is shown by microscopy images in Fig.2. Thermoplastic interleaves are observed as lighter regions at the interfaces. The images of the control samples (Fig.2a) show uniform interfaces with the drill site introducing delamination at the exit end. The microscopy view in Fig.2b may indicate partial infusion of the thermoplastic interleaves into each adjacent ply, since no clear boundary can be seen between the thermoplastic and fibres. This is expected given that the curing temperature is higher than the melting temperature of interleaves. However, the extra material still caused the thickness of the interleaved region to become larger than that of the control samples by ~0.36 mm, (thicknesses are given in Section 2.1). After the reheating treatment (Fig.2c), the thermoplastic at the internal region of the specimen don't appear to have any significant change however near the sample edges or the hole site, part of the thermoplastic material leaked out, more clearly shown in Fig.3. The reheated samples had a nominal thickness of 2.6 mm with ~0.15 mm reduction due the loss of thermoplastic.

The aim of this investigation was to assess the local delamination near the drilled hole site. The push-out delamination at the 45°/90° interface at the drill bit exit side is of particular interest since this is the location where worst damage usually occurs [5]. To observe this, cross section of the sample was made at 45° as shown in the schematic in Fig.2. The largest peel can be seen on the surface 45° ply in Fig.2a. Similar damage (local delamination) is not observed on any other ply interface. (Note, more severe damage including significant delamination may occur with less accurate drilling procedure, e.g. slow rpm or non-carbide drills). Comparison with the control specimen (Fig. 2a), the non-reheated interleaved specimen (Fig. 2b) shows the extent of the ply peel to be smaller. Scope of this investigation was to see whether any delamination damage near the drill site can be repaired. As shown in Fig.2c after the reheating treatment, the initial damage around the open hole was healed with any minor crack and gap among fibres and plies, have been filled with thermoplastic. Although for the stacking sequence studied here, the initial drilling damage on the surface ply does not appear to have much influence on the tensile strength of the specimen, according to the analysis detailed in Section 2.4, the behaviour may be different when the structure is subjected to tensile loads in the direction of the surface ply fibres. Additionally, when the laminate is subjected to the static/cyclic flexure or torsional load, this healing treatment may be an effective approach to improve its structural integrity.

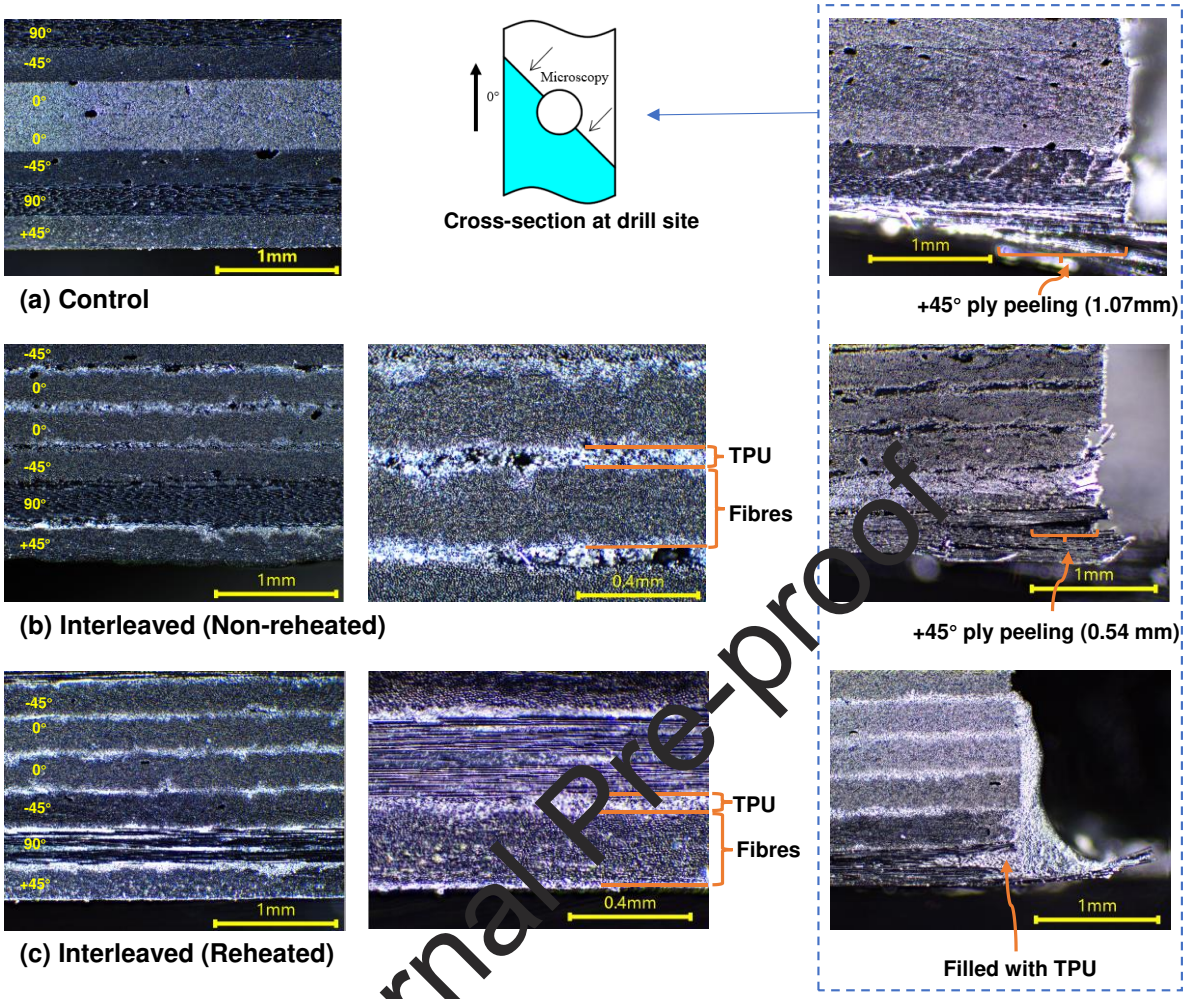

Fig.2 Cross-section microscopy images of control and TPU interleaved samples. Drill site location are shown on the rightmost images

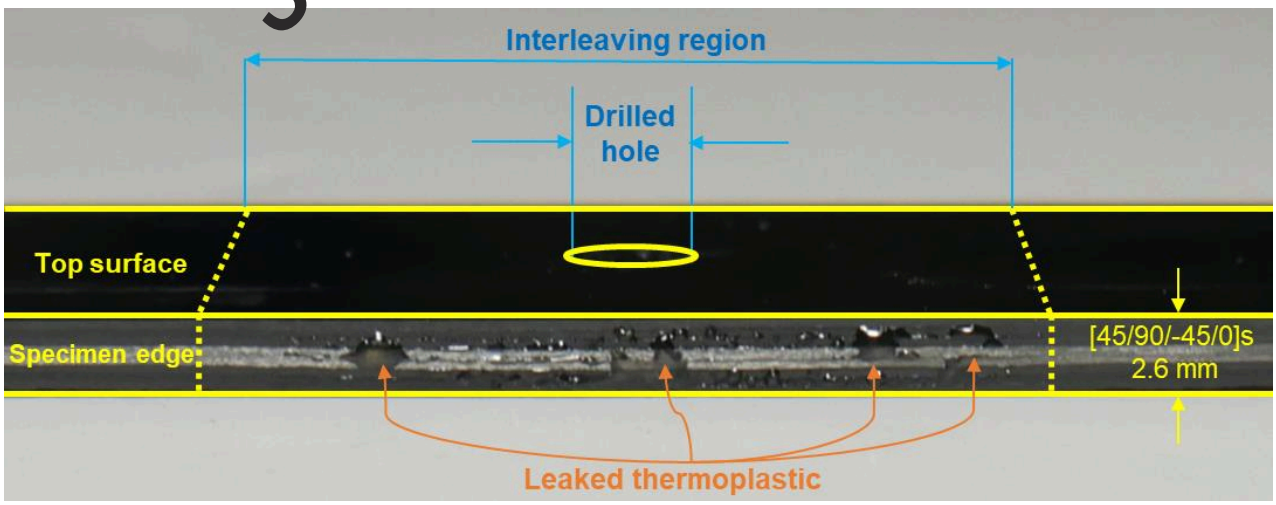

Fig.3 Side view of a reheated interleaved specimen showing the thermoplastic leaking from the specimen edges

2.4 Results

The load-displacement results of the control and interleaved samples are presented in Fig.5. During the full load cycle of the open hole notched specimen, the sample exhibits several stages towards the ultimate failure. Initial linear-elastic region which lasts approximately up to 10kN is the portion of the test where no damage is present. From 10kN towards the first load drop is referred to as quasi-linear stage since here the surface ply splitting (matrix cracks) was observed as shown in Fig.4. The first and the final load drops are referred to as tensile failure and ultimate failure respectively.

Fig.4 The surface ply (+45°) splitting during loading process
(Recorded by a 4K DSLR camera)

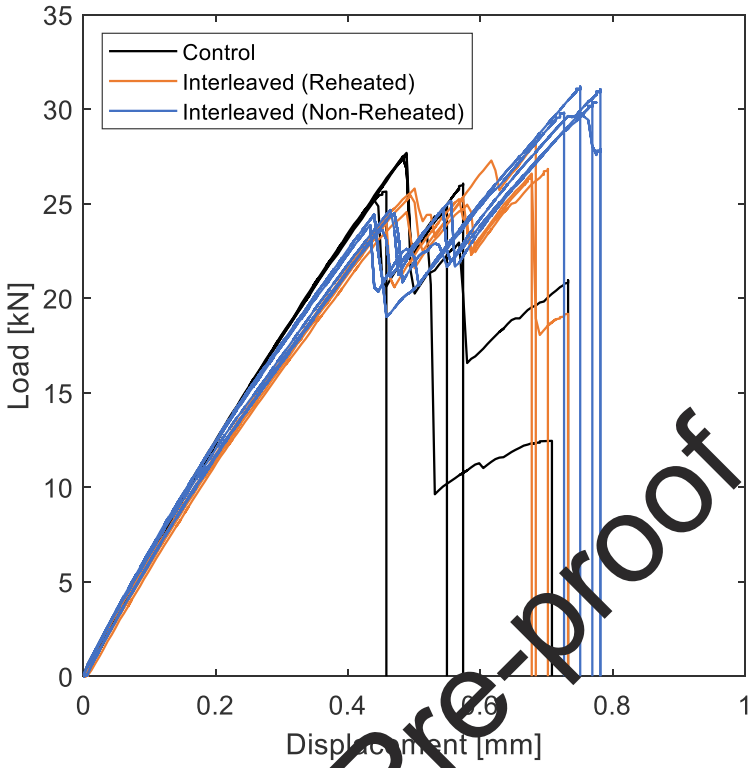

Fig.5 Load-displacement results of control and interleaved open hole notched samples

During the initial loading process, the DIC image (Fig.6) which is of the top surface with the +45° ply, reveal a path of high shear strain tangential to the hole boundary across the specimen orientated at 45° to the loading direction. The increasing shear strain leads to ply splits at this region. These splits along with 90° and -45° ply splits which may occur internally cause minor non-linearity as seen in the load-displacement curve before the first load drop in each sample. Detailed study of the failure mechanism and their corresponding features on the load - displacement plot will be presented in Section 3.2.

The control samples appear to have higher tensile failure load (first load drop) and higher stiffness in the quasi-linear stage relative to the interleaved samples. The tensile failure load for the control sample is the maximum load, with the secondary and ultimate failure occurring at lower load. The interleaved samples exhibit on average lower tensile failure load (first load drop), however, the samples exhibit further load-carrying capacity with the ultimate failure

load for both batches of interleaved samples being higher. Both the ultimate failure load and displacement of the non-reheated interleaved specimens are higher than those of the reheated interleaved specimens.

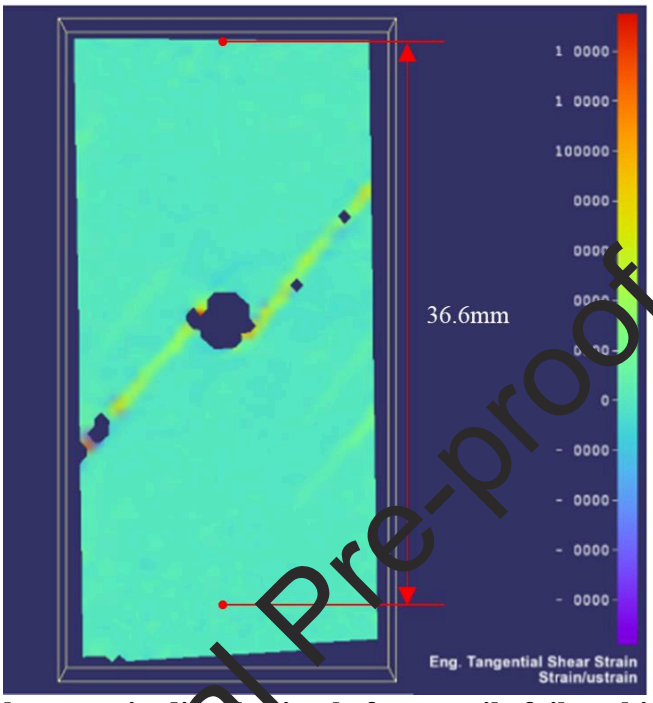

Fig.6 DIC image of shear strain distribution before tensile failure highlighting the displacement measurement points at distance of 36.6 mm

The comparisons of key parameters are shown in Fig.7. The control specimens showed the highest tensile failure load but the lowest ultimate failure load and displacement as well as the lowest overall work of fracture until ultimate failure. With the addition of the interleaves, the overall stiffness of the sample appears to have reduced slightly with the tensile failure load dropping significantly. This is counterintuitive since this first load drop was assumed to be delamination dominated thereby not clear why this value has reduced with the addition of interleaves. Compared with the control specimens, this first load drop is lower for the non-reheated interleaved samples however it is partially recovered after re-heat treatment. The ultimate failure load of the non-reheated interleaved specimens is higher than the control samples. However after re-reheating treatment, interleaved samples reached similar ultimate

failure load as the control samples. Overall, the work of fracture of the open hole specimens increased significantly with the addition of interleaves but the increase was lower for the reheated specimens. Same trend can be seen for the displacement at ultimate failure. Results here suggest that the OHT performance can be improved with the addition of thermoplastic interleaves however the re-heating treatment of the interleaved samples does not provide additional performance gains but in fact reduces the ultimate failure strength of the interleaved specimens significantly. These results suggest that interfacial stiffness, toughness, and strength have a strong influence on the sequence of failure mechanisms in a composite laminate. With a high toughness and low stiffness of the interface introduced by the thermoplastic interleaves, the feature of a lower initial load drop but an overall higher ultimate failure strength was presented by the notched structure. Observation of the pulled-out ply sections of the tested interleaved samples revealed patched residue of the TPU material on the surface. This would be indicative of the TPU film splitting during delamination of the interface representative of cohesive failure rather than adhesive failure. Similar failure response was reported by Pappa et. al. [14] who also observed cohesive failure in their TPU interleaved DCB samples. Detailed study of these behaviours will be made in Section 3.3 with the help of numerical analysis.

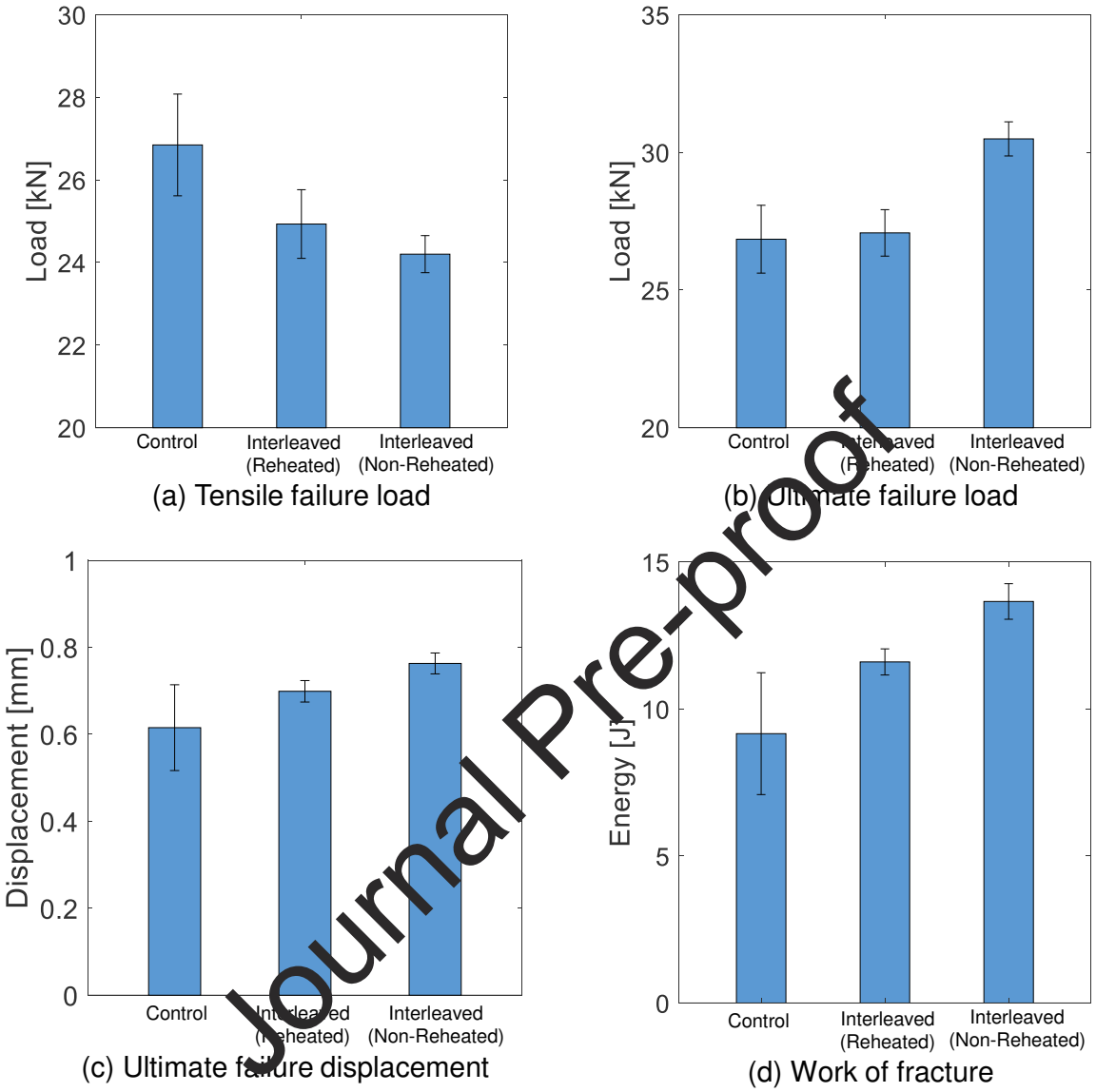

Fig.7 Average value for key parameters (a) Tensile failure load (b) Ultimate failure load (c) Displacement for ultimate failure (d) Work of fracture until ultimate failure

3 Numerical analysis

The numerical analysis in this section is organised into two parts. In part 1, Section 3.1 and Section 3.2, explained the model setup and modelling results to verify against the experimental data. This ensures that the modelling procedure works correctly to capture all the failure mechanisms accurately. In part 2, sensitivity study was carried out in Section 3.3 by using the modelling procedure with different interfacial properties for the laminate interfaces to

understand, with clarity, what influence these properties have on the failure response of the open-hole composites.

3.1 Model setup and verification

Following the methodology from the work of Hallett et. al [4], numerical models of the open hole composite specimen were created in FE with cohesive zone models utilised to represent the different damage mechanism present in the composite system from matrix cracking, fibre fracture and delamination. All the FE models were made in ABAQUS and solved with explicit solver on high performance computing system. A ply-by-ply modelling approach was used to represent the 8-ply laminates however simplified to a 4-ply ([45/90/-45/0]) laminates with symmetry boundary condition applied to the surface of the internal 0° ply. Each model consists of ~40,000 0.5 mm SC8R continuum shell elements for the full laminate. The laminate mechanical properties are given in Table 2, collected from material data sheet from the supplier as well as the properties of similar material.

Ply splits (matrix cracks) were introduced by method of intra-ply cohesive contact as shown in Fig.8. The modelling of specific split locations is supported by experimental observation as shown in Fig.4. Furthermore, this method was investigated by Hallet et al.[4] and its capability of replicating the damage process of composite laminates has been shown to be effective. The split paths were pre-set at 1 element length away from the hole edge to avoid extreme element distortion which will produce incorrect results. To replicate the 0° ply tensile fracture, cohesive contact approach was found to produce instability in the fracture profile, with few contact nodes that remain attached when majority have failed. This gave incorrect failure sequence. To overcome this, cohesive elements (COH3D8) were utilised to replicate the fibre fracture path across the full width on 0° ply only. Both these cohesive models use bi-linear cohesive law to represent the damage initiation and propagation with mixed mode behaviour represented with either B-K law with exponent of 2.1 or power law with exponent of 1. For this study most

cohesive contact failure is either Mode I or Mode II dominated and thereby the mixed mode settings will have negligible influence on the results.

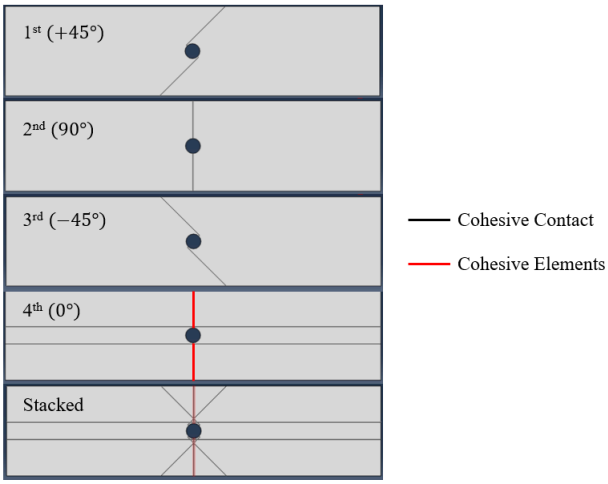

Fig.8 Pre-set intra-ply damage paths of the FE model

Cohesive contacts were also applied for the interfaces between each adjacent plies to represent delamination. For the interleaved region the 24×25 mm area as shown in Fig.1 was assigned with the interleaved cohesive contact properties that are listed in Table 4 as the input parameter. Readers should note that the interleaved material is not explicitly modelled. Only its effect on the laminate interface is captured using the cohesive zone model (CZM), which is a procedure that has been shown accurate to represent interleaved interfaces, see Saghafi et. al. [25] , Giuliese et. al. [26] and Hosseini et. al. [27]. Additionally, Tserpes and Koumpias [28] have compared the capability of CZM to simulate delamination of interleaved interfaces by comparing their results with models which use solid elements with continuum damage mechanics (CDM) to simulate failure of the interleaf material at the interface of double cantilever beam (DCB) specimens. They showed that both CZM and CDM methods are equally reliable in the prediction of delamination failure with CZM being more computationally efficient.

Note, given that interfacial toughness properties were not available for this material system, values used are based on initial calibration exercises and related studies [14]. Two delamination

toughness levels are applied for the control models to replicate the potential manufacturing variation, one with high toughness and one with low toughness but both with identical cohesive stiffness and strength. Interleaved specimen is represented by one model to investigate the influence of the interfacial mechanical properties introduced by the thermoplastic interleaves. Due to the modelling procedure used, it is not possible to create a model to differentiate between the non-reheated and reheated samples. This is due to the reheating treatment resulting in only a small change in failure load values as shown in Fig.5, rather than significant damage process variations. The cohesive stiffness of the interfaces in the interleaved model is lowered to replicate the reduced stiffness of the thermoplastic interleaves, as seen in the reduced specimen stiffness of the interleaved samples in Fig.5. The locations of the different interface cohesive contact regions are shown in Fig.9. The full boundary conditions applied including the symmetry condition at the 0° surface are annotated as well.

The Mode I cohesive property for the ply fibre fracture were set with strength (SI) to the value of the ply strength in the fibre direction (see Table 2) and GIC set to the fracture toughness associated with composite material in the longitudinal fibre direction. This value ranges anywhere between 10kJ/m^2 to 100kJ/m^2 [29] and was found in this study not to make significant difference for values >10 kJ/m^2. Since there is no fibre fracture in the transverse direction, its transverse cohesive strength (SII) was set to an arbitrary large value to remove the activation of this behaviour from the simulation. In doing so the cohesive element will only fail to represent ply tensile fracture only.

Table 4 Cohesive contact properties (S: Interfacial Strength G: Interfacial Toughness K: Cohesive stiffness)

		SI [MPa]	SII [MPa]	GIC [kJ/m^2]	GIIC [kJ/m^2]	KI, KII [N/mm^3]
Interface	Control (High Toughness)	30	220	0.4	0.9	1.00E+05
	Control (Low Toughness)	30	220	0.3	0.7	1.00E+05
	Interleaved	20	60	0.5	1.0	1.00E+03
Ply strength	Xt	2,550	10,000	10.0	10.0	1.35E+05，7E+03

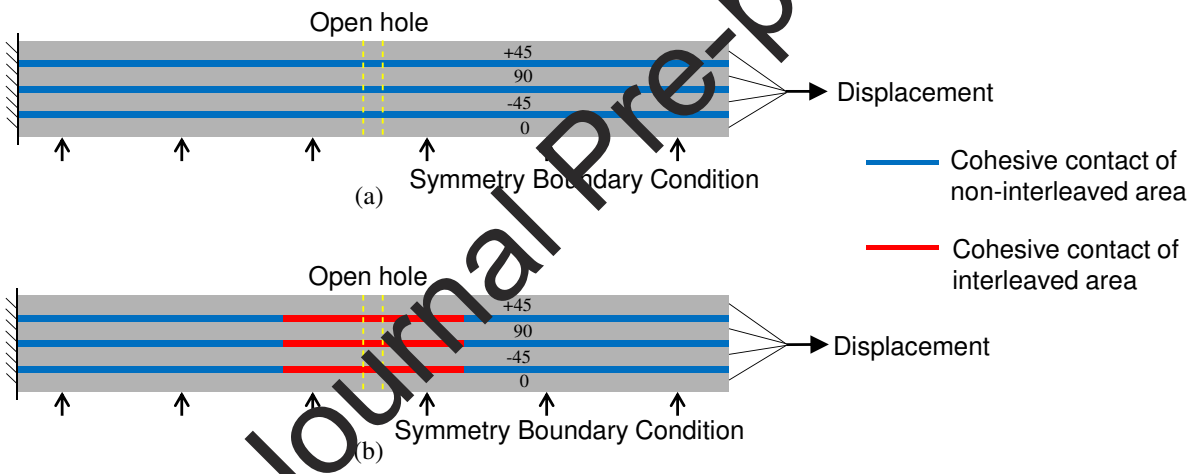

Fig.9 Interfacial interaction of FE model (Not scaled) (a) Control model (b) Interleaved model

3.2 Model verification results

Numerical analysis load-displacement results are presented in Fig.10. The details of the failure mechanisms that contribute the load-displacement features are shown Fig.11. Results showcase general good correlation against experimental data. The control models have higher stiffness and tensile failure load than the interleaved model. It appears that the control model with higher interfacial toughness reached a higher tensile failure load with full fibre fracture failure on both

sides of the hole (Fig.11a). The control model with lower interfacial toughness shows slightly lower tensile failure load but with only half of the 0° ply exhibiting fibre fracture (Fig.11b). This means the sample was capable to carry load after the tensile failure until the second part of the 0° ply failed. The model of interleaved specimen has a lower tensile failure load and stiffness than both the control models. However, after two relatively small load drops, the specimen was still capable to carry the increasing tensile load and reached the highest value among all the specimens before the ultimate failure by full fibre fracture on both sides of the hole (Fig.11c). According to the FE analysis in this study and the similar feature from other reports [3], it is shown that the -45°/0° delamination has caused the relatively small initial load drops seen in the interleaved samples.

The initial non-linearity across the three cases was clearly caused by the intra-ply splits in all the plies. However, it was found that the 0° ply splits contribute directly to the ultimate load-carrying ability of the composite laminate. This is because 0° ply splits reduced the stress concentration on the 0° ply fibres surrounding the open hole, thus delaying the ultimate failure. Another interesting behaviour observed is with samples where half fibre fractures occur in the 0° plies after tensile failure (first load drop) as shown in Fig.11b. Simulations indicate that accompanied by the first load drop of both control models, local delamination was exhibited at the fibre fracture site, where the high interfacial toughness model showed the least amount of local delamination. These results indicate the strong influence of the interfacial fracture toughness, strength, and stiffness on the failure sequence of the open hole specimens. The two different responses seen in the experimental control samples (Fig.11a,b) showcase this behaviour. Perhaps small variations in the material fracture toughness properties can result in the differences in the overall mechanical response.

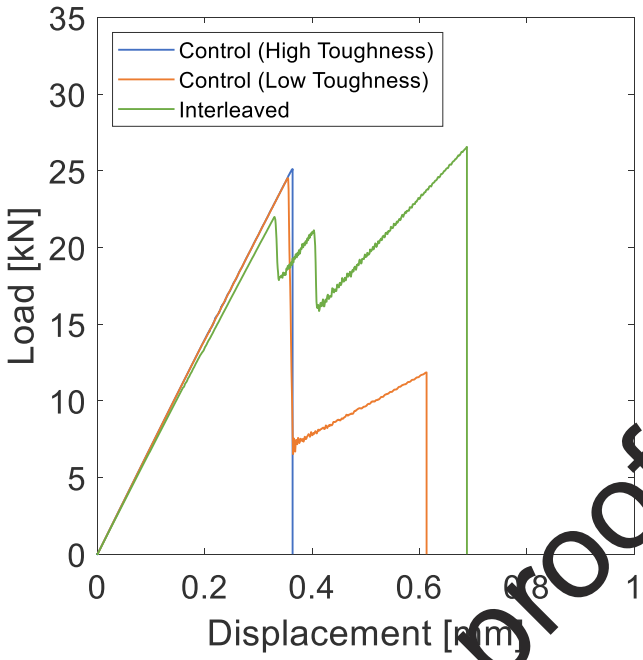

Fig.10 Load-displacement curves from FE simulation

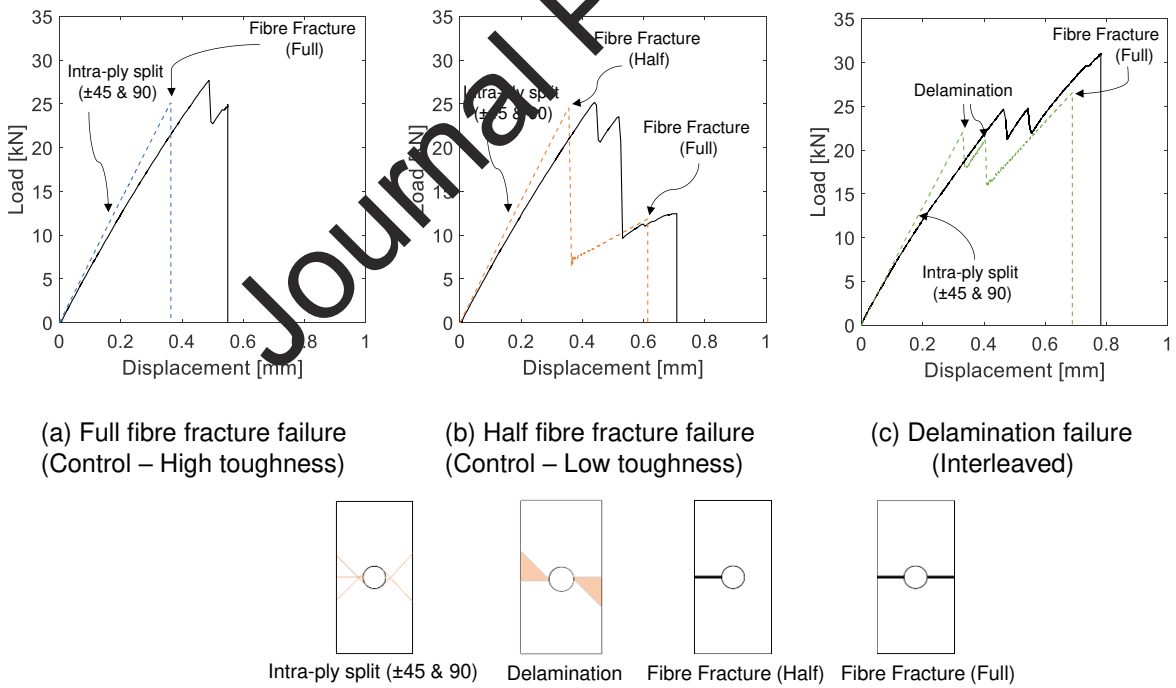

Fig.11 Comparison of FE (dashed line) and tension test (solid line) results (Schematics are annotated for FE)

Observing the extent of the damage prior to the tensile failure (first load drop) shown in Fig.12 it is evident that the interleaved model showed the longest 0° split. This may be due to the

lower interfacial strength of the interleaved model which leads to weaker constraint among fibres and plies. This also led to a larger delamination area at the -45°/0° interface as shown in the same picture. These initial large damage formations caused stress redistribution releasing the high stress concentration at the open hole boundary, protecting the 0° fibres from early failure.

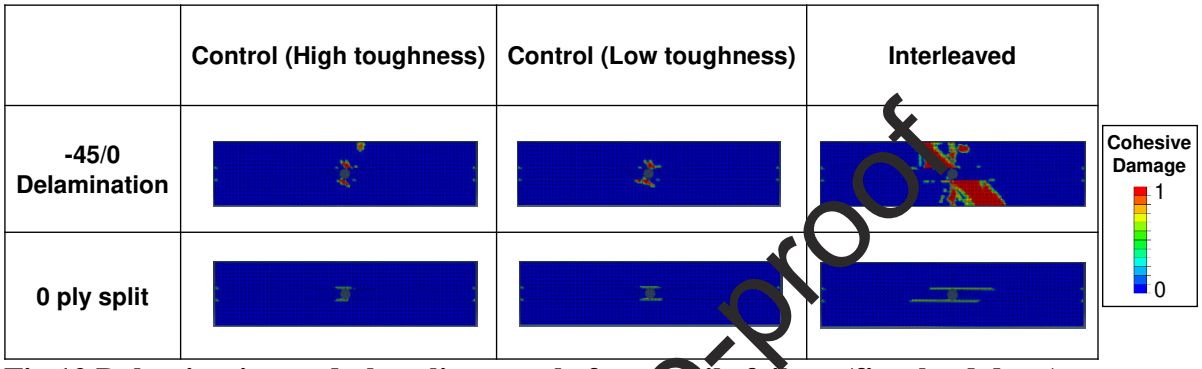

Fig.12 Delamination and ply split status before tensile failure (first load drop)

It has been found no matter how the 0° fibres fail, all load drops are accompanied by significant and rapid delamination propagation at the -45°/0° interface. Hence, the delamination at the interfaces adjacent to 0° plies are the predominant factor for the onset of tensile failure. It implies that the stronger the bonding performance of this interface, the more likely 0° fibres will fail with the onset of delamination. Furthermore, 0° fibres can also be damaged by the shock stress formed after sudden delamination growth. This sudden delamination growth can be mitigated through higher interfacial toughness and lower stiffness. Hence, the 0° fibres are protected from the shock stress so that they retain their integrity to carry the increasing tensile load.

3.3 Failure mechanisms sensitivity analysis of varying interleaf properties

This study has demonstrated the importance of the interfacial properties on the sequence of the failure mechanism observed in the tensile behaviour of open hole composite materials. In this section, this concept will be analysed in detail to understand how changes to the interfacial

strength and interfacial toughness affect the failure mechanism sequence and thus influence the overall composite open hole tensile strength.

Table 5 Interfacial properties for sensitivity study

Specimen	SI [MPa]	SII [MPa]	GIC [kJ/m^2]	GIIC [kJ/m^2]	KI, KII [N/mm^3]
High strength, high toughness (HSHT)	250	250	1.0	3.0	1.00E+05
High strength, low toughness (HSLT)	250	250	0.1	0.4	1.00E+05
Low strength, high toughness (LSHT)	20	20	1.0	3.0	1.00E+05
Low strength, low toughness (LSLT)	20	20	0.1	0.4	1.00E+05

Shown in Table 5, four sets of interfacial contact properties were assigned to the entire interfaces of four models, which have the same dimensions and stacking sequences as introduced in Section 2.1 and Section 3.1. The contact properties have fixed upper and lower strength and toughness values, which were intentionally set to very high or very low values to present a high contrast comparison of their influence on the overall mechanical response. The four cases are high strength, high toughness (HSHT), high strength, low toughness (HSLT), low strength, high toughness (LSHT) and low strength, low toughness (LSLT).

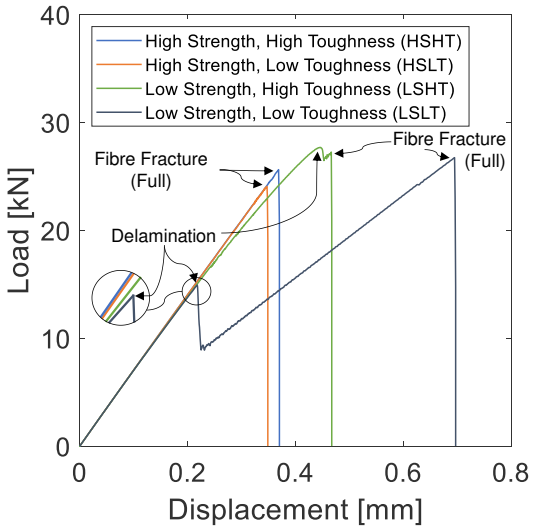

Fig.13 Load-displacement curves of the interface sensitivity study with the failure mechanisms at each load drop

The simulation results of the open hole tension models are shown in Fig.13. By comparing the slope of each curve at the quasi-linear stage, both models with higher interfacial strength show more constant stiffness than the models with lower interfacial strength which have the stiffness reduced slightly. The reduced stiffness is the result of delamination propagation at -45°/0° interface prior to the first load drop. The comparison of tensile failure load between LSHT and LSLT indicates that, higher interfacial toughness delays and stabilises the delamination propagation, avoiding early tensile failure which can be seen in LSLT caused by a sudden large scale -45°/0° delamination.

Influence of interfacial strength can be seen between HSHT and LSHT models, where overall improvement to the failure response can be achieved with a lower interfacial strength. This is because reduced interfacial strength allows for early small scale local delamination which has the effect of reducing the stress concentration around the hole. This occurs because 0° splits near the open hole appear along with the local delamination, which release the shear stresses on the 0° fibres from both the adjacent 0° and the -45° ply as well as the inner-ply fibres, thereby delaying early failure compared with the model with high interfacial strength. The extent of the slow and stable delamination growth is presented in Fig.15, far more than those from high strength interfaces shown in Fig.14. Hence, higher interfacial strength does not always give the specimen the highest tensile strength.

Comparing LSLT and HSLT it is evident that interfacial strength improves the open hole performance with higher tensile strength capability. However, LSLT did have overall higher ultimate strength compared with HSLT.

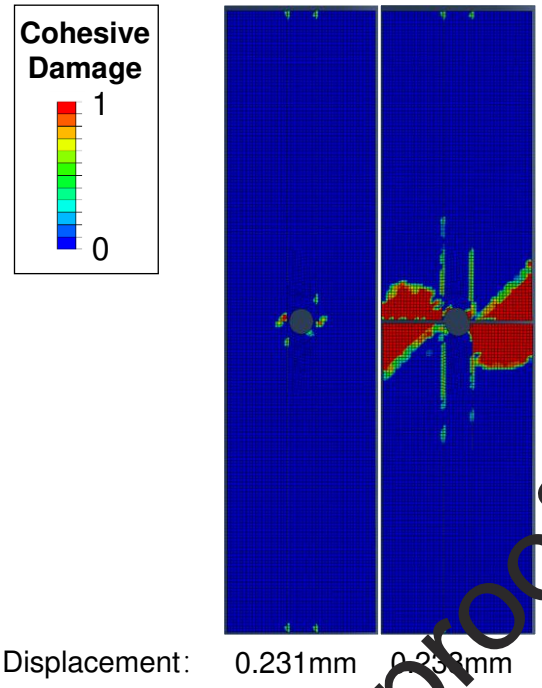

Fig.14 Delamination propagation of high strength, high toughness (HSHT) type model

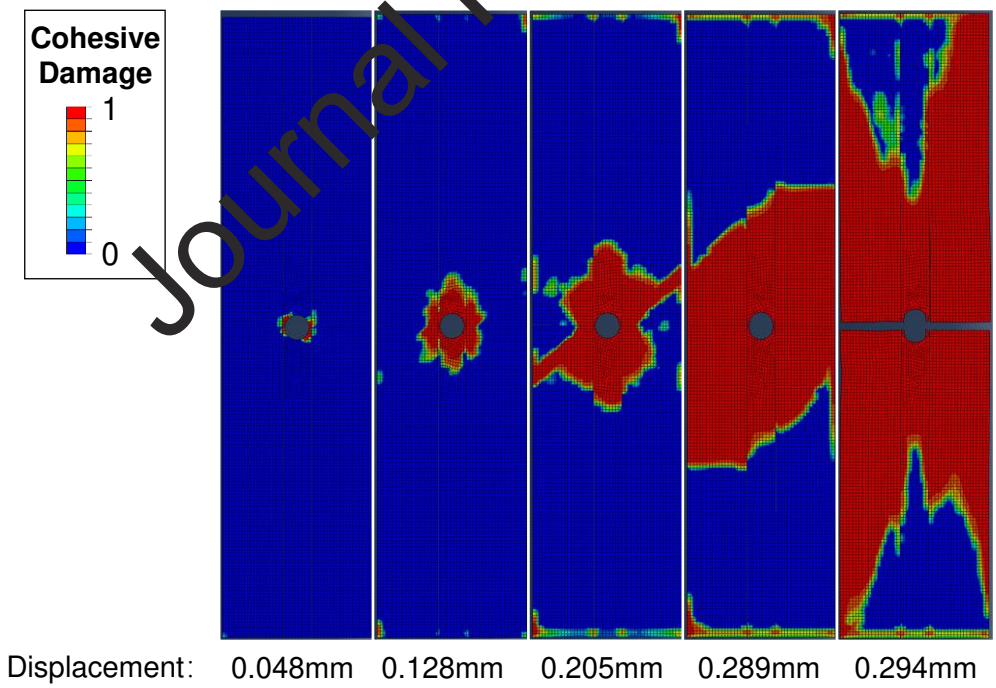

Fig.15 Delamination propagation of low strength, high toughness (LSHT) type model

4 Discussion and conclusions

In this study, the performance of open hole CFRP composites under tensile load, has been analysed in detail to understand the influence of thermoplastic interleaves on their behaviour.

The open hole tensile failure of quasi-isotropic ($[45/90/-45/0]_S$) specimens is dominated by the delamination of 0°/-45° interface. The increase in interfacial toughness and decrease in interfacial strength provided by the interleaves helped to slow the propagation of the delamination and thus avoid the early onset of fibre fracture of the 0° plies.

The thermoplastic interleaves produced a softer interface thereby causing an overall lower stiffness of the sample. The effect of this lowered interfacial stiffness and strength led to early 0° ply splits thus reducing the stress concentration on the 0° ply and preventing early loss of the load carrying capability of the specimen. However, this did cause an early load drop which was due to onset of delamination and not because of 0°ply failure. Thereby both interleaved batches maintained the 0° ply integrity post first load drop and thus were capable to sustain higher overall ultimate strength than the control samples.

Thermoplastic interleaves provide the capability to heal any delamination damage that may have formed because of hole drilling through the application of heat and pressure. The interleaved specimens which had reheating treatment applied showed higher tensile strength than the non-reheated specimens, perhaps brought about by reducing any micro cracks or delamination that may have formed. Consequently, it might cause early failure of small portion of 0° fibres resulting in a relatively low ultimate strength. Attentions on how to prevent thermoplastic leaking during the reheating treatment need to be paid, in order to remain the high interfacial toughness feature.

Numerical simulations helped to identify the relationship of open-hole notched composites' damage process to multiple factors, including the interfacial strength, stiffness, and toughness. Variations to any of these parameters can lead to completely different structural performance as a result of the changes to the failure mechanism sequence. A major finding here was on the effect of ply interface properties on the reduction of stress concentrations around the hole for the 0° ply. By having an interface with identical toughness but lower interfacial strength, the

open hole strength can be significantly increased as the stress concentration around the hole can be reduced.

To manipulate composite's overall mechanical response by adjusting interfacial properties, interleaving approach does not only need to improve the interfacial toughness but also change the interfacial stiffness as well. With use of thermoplastic interleaves shown here, the growth of local delamination through the interleaves prior to ultimate failure results in lowered specimen stiffness which indicates a permanent deformation. This may provide opportunity, through reheating treatment, to recover the structural integrity of the open hole specimens after overloading and perhaps provide mechanism to improve and prolong the use of composite components with holes.

Furthermore, interfacial toughening may not be necessary at all the interfaces, since selective interleaves at critical interfaces may help to improve the mechanical performance of the open hole composites which will depend on the load case and the stacking sequence. These concepts will be interesting to pursue in future studies on this topic.

References

[1] J. Xu, C. Li, S. Mi, Q. An, M. Chen, Study of drilling-induced defects for CFRP composites using new criteria, Compos. Struct. 201 (2018) 1076–1087. https://doi.org/10.1016/j.compstruct.2018.06.051.

[2] M.R. Wisnom, S.R. Hallett, The role of delamination in strength, failure mechanism and hole size effect in open hole tensile tests on quasi-isotropic laminates, Compos. Part A Appl. Sci. Manuf. 40 (2009) 335–342. https://doi.org/10.1016/j.compositesa.2008.12.013.

[3] B.G. Green, M.R. Wisnom, S.R. Hallett, An experimental investigation into the tensile strength scaling of notched composites, Compos. Part A Appl. Sci. Manuf. 38 (2007) 867–878. https://doi.org/10.1016/j.compositesa.2006.07.008.

[4] S.R. Hallett, B.G. Green, W.G. Jiang, M.R. Wisnom, An experimental and numerical investigation into the damage mechanisms in notched composites, Compos. Part A

Appl. Sci. Manuf. 40 (2009) 613–624. https://doi.org/10.1016/j.compositesa.2009.02.021.

[5] U.A. Khashaba, Delamination in drilling GFR-thermoset composites, Compos. Struct. 63 (2004) 313–327. https://doi.org/10.1016/S0263-8223(03)00180-6.

[6] D.F. Liu, Y.J. Tang, W.L. Cong, A review of mechanical drilling for composite laminates, Compos. Struct. 94 (2012) 1265–1279. https://doi.org/10.1016/j.compstruct.2011.11.024.

[7] N. Sela, O. Ishai, Interlaminar fracture toughness and toughening of laminated composite materials: a review, Composites. 20 (1989) 423–435. https://doi.org/10.1016/0010-4361(89)90211-5.

[8] M. Yasaee, I.P. Bond, R.S. Trask, E.S. Greenhalgh, Mode I interfacial toughening through discontinuous interleaves for damage suppression and control, Compos. Part A Appl. Sci. Manuf. 43 (2012) 198–207.

[9] M. Yasaee, I.P. Bond, R.S. Trask, E.S. Greenhalgh, Mode II interfacial toughening through discontinuous interleaves for damage suppression and control, Compos. Part A Appl. Sci. Manuf. 43 (2012) 121–128.

[10] A. Aksoy, L.A. Carlsson, Interlaminar shear fracture of interleaved graphite/epoxy composites, Compos. Sci. Technol. 43 (1992) 55–69. https://doi.org/10.1016/0266-3538(92)90133-N.

[11] D. Quan, F. Bologna, G. Scarselli, A. Ivankovic, N. Murphy, Interlaminar fracture toughness of aerospace-grade carbon fibre reinforced plastics interleaved with thermoplastic veils, Compos. Part A Appl. Sci. Manuf. 128 (2020) 105642. https://doi.org/10.1016/J.COMPOSITESA.2019.105642.

[12] C.H. Wang, K. Sidhu, T. Yang, J. Zhang, R. Shanks, Interlayer self-healing and toughening of carbon fibre/epoxy composites using copolymer films, Compos. Part A Appl. Sci. Manuf. 43 (2012) 512–518. https://doi.org/10.1016/j.compositesa.2011.11.020.

[13] K. Pingkarawat, C.H. Wang, R.J. Varley, A.P. Mouritz, Self-healing of delamination cracks in mendable epoxy matrix laminates using poly[ethylene-co-(methacrylic acid)] thermoplastic, Compos. Part A Appl. Sci. Manuf. 43 (2012) 1301–1307. https://doi.org/10.1016/j.compositesa.2012.03.010.

[14] E.J. Pappa, E.D. McCarthy, C.O. Brádaigh, Optimisation of carbon fibre reinforced polymer composites with a thin embedded polyurethane film, ICCM Int. Conf. Compos. Mater. 2019-Augus (2019).

[15] C. Cheng, C. Zhang, J. Zhou, M. Jiang, Z. Sun, S. Zhou, Y. Liu, Z. Chen, L. Xu, H. Zhang, M. Yu, Improving the interlaminar toughness of the carbon fiber/epoxy composites via interleaved with polyethersulfone porous films, Compos. Sci. Technol. 183 (2019). https://doi.org/10.1016/j.compscitech.2019.107827.

[16] S.G. Marino, F. Mayer, A. Bismarck, G. Czél, Effect of Plasma-Treatment of Interleaved Thermoplastic Films on Delamination in Interlayer Fibre Hybrid Composite Laminates, Polym. 2020, Vol. 12, Page 2834. 12 (2020) 2834. https://doi.org/10.3390/POLYM12122834.

[17] X. Qian, O.G. Kravchenko, D. Pedrazzoli, I. Manas-Zloczower, Effect of polycarbonate film surface morphology and oxygen plasma treatment on mode I and II fracture toughness of interleaved composite laminates, Compos. Part A Appl. Sci. Manuf. 105 (2018) 138–149. https://doi.org/10.1016/J.COMPOSITESA.2017.11.016.

[18] ASTM, D3039/D3039M-17 Standard test method for tensile properties of polymer matrix composite materials, Am. Soc. Test. Mater. (2014) 1–13. https://doi.org/10.1520/D3039.

[19] ASTM, D5766/D5766M-11 Standard Test Method for Open-Hole Tensile Strength of Polymer Matrix Composite, Am. Soc. Test. Mater. 11 (2011) 1–7. https://doi.org/10.1520/D5766.

[20] Toray CA Inc., T700S Technical Data Sheet, (2005) 2.

[21] Easy Composites Ltd, XC130 300g Unidirectional Prepreg Carbon Fibre 300mm, (n.d.). https://www.easycomposites.co.uk/xc130-300g-unidirectional-prepreg-carbon-fibre (accessed August 28, 2021).

[22] Chinese Aeronautical Establishment, Composite Structural Design Manual, 1st ed., 2001.

[23] J. Tomblin, J. Sherraden, W. Seneviratne, K.S. Raju, A - Basis and B - Basis Design Allowables for Epoxy Based Prepreg TORAY T700GC-12K-31E/#2510 Unidirectional Tape [US Units], Adv. Gen. Aviat. Transp. Exp. (2002) 1–214.

[24] Shenzhen Tunsing Plastic Products Co. Ltd., Technical Datasheet of DS8614, (2021).

[25] H. Saghafi, S.R. Ghaffarian, T.M. Brugo, G. Minak, A. Zucchelli, H.A. Saghafi, The effect of nanofibrous membrane thickness on fracture behaviour of modified composite laminates – A numerical and experimental study, Compos. Part B Eng. 101 (2016) 116–123. https://doi.org/10.1016/J.COMPOSITESB.2016.07.007.

[26] G. Giuliese, R. Palazzetti, F. Moroni, A. Zucchelli, A. Pirondi, Cohesive zone modelling of delamination response of a composite laminate with interleaved nylon 6,6

nanofibres, Compos. Part B Eng. 78 (2015) 384–392. https://doi.org/10.1016/J.COMPOSITESB.2015.03.087.

[27] M.R. Hosseini, F. Taheri-Behrooz, M. Salamat-talab, Mode I interlaminar fracture toughness of woven glass/epoxy composites with mat layers at delamination interface, Polym. Test. 78 (2019) 105943. https://doi.org/10.1016/J.POLYMERTESTING.2019.105943.

[28] K.I. Tserpes, A.S. Koumpias, Comparison between a cohesive zone model and a continuum damage model in predicting mode-I fracture behavior of adhesively bonded joints, C. - Comput. Model. Eng. Sci. 83 (2012) 169–181. https://doi.org/10.32604/cmes.2012.083.169.

[29] M.J. Laffan, S.T. Pinho, P. Robinson, L. Iannucci, A.J. McMillan, Measurement of the fracture toughness associated with the longitudinal fibre compressive failure mode of laminated composites, Compos. Part A Appl. Sci. Manuf. 43 (2012) 1930–1938. https://doi.org/10.1016/j.compositesa.2012.04.009.

Tianqi Zhang: Investigation, Data curation, Software, Formal analysis, Writing-Original draft preparation, Visualization, Validation

Mehdi Yasaee: Conceptualization, Methodology, Supervision, Software, Writing-Reviewing and Editing

Declaration of interests

☒ The authors declare that they have no known competing financial interests or personal relationships that could have appeared to influence the work reported in this paper.

☐ The authors declare the following financial interests/personal relationships which may be considered as potential competing interests:

2022-06-26

Influence of thermoplastic interleaves and its healing effect on the failure mechanisms of open-hole notched composite laminates

Zhang, Tianqi

Elsevier

Zhang T, Yasaee M. (2022) Influence of thermoplastic interleaves and its healing effect on the failure mechanisms of open-hole notched composite laminates. Composites Science and Technology, Volume 227, August 2022, Article number 109597

https://doi.org/10.1016/j.compscitech.2022.109597